

³⁵Cl Quadrupole Relaxation Study on Cs₂[Au(I)Cl₂][Au(III)Cl₄] and Cs₂[Ag(I)Cl₂][Au(III)Cl₄]

A. Ishikawa, M. Kurasawa, K. Kurasawa, A. Sasane, R. Ikeda^a, and N. Kojima^b

Department of Chemistry, Faculty of Science, Shinshu University, Matsumoto 390-8621, Japan

^a Department of Chemistry, University of Tsukuba, Tsukuba 305-8751, Japan

^b Department of Basic Science, Graduate School of Arts and Sciences, The University of Tokyo, Tokyo 153-8902, Japan

Reprint requests to Dr. A. I.; Fax: +81-263-37-2559, E-mail: ishikawa@ripms.shinshu-u.ac.jp

Z. Naturforsch. **57 a**, 348–352 (2002); received January 23, 2002

Presented at the XVth International Symposium on Nuclear Quadrupole Interactions, Hiroshima, Japan, September 9-14, 2001.

Two ³⁵Cl NQR spin echo signals, $\nu_{Q1} = 17.28$ MHz (Au(I)-Cl) and $\nu_{Q2} = 27.10$ MHz (Au(III)-Cl), have been observed at 77 K from two samples of Cs₂[Au(I)Cl₂][Au(III)Cl₄] prepared differently. The resonances resulted at the same frequencies but with different line widths. Cs₂[Ag(I)Cl₂][Au(III)Cl₄] yielded a singlet, $\nu_{Q2} = 27.96$ MHz, at 77 K. The three samples gave rise to ESR signals indicating the presence of paramagnetic Au(II) or Ag(II) sites with low concentration. ³⁵Cl NQR spin-lattice relaxation time T_{1Q} measurements revealed that only the reorientational motions of the anions [Au(III)Cl₄]⁻ are excited at high temperatures.

Key words: ³⁵Cl NQR Spin-lattice Relaxation; Mixed-valence Complex; Reorientational Motion; Lattice Vibration; ESR.

Introduction

The mixed-valence complexes M₂[Au(I)X₂]-[Au(III)X₄] (M = Rb and Cs; X = Cl, Br, and I) have attracted many workers, cf. [1]. In a previous paper [2], we reported that tetragonally distorted perovskite type Cs₂[Au(I)Cl₂][Au(III)Cl₄] polycrystals yielded two ³⁵Cl NQR lines, $\nu_{Q1} = 17.28$ and $\nu_{Q2} = 27.10$ MHz at 77 K, in accordance with the crystal structure, I4/mmm [3 - 5]. These signals were assigned to the two kinds of Cl atoms in the crystal: ν_{Q1} to Cl-Au(I) and ν_{Q2} to Cl-Au(III). The estimate of the charge distribution in the complex anions clarified that the charge transfer interactions between the anions are weak in this mixed-valence complex.

However, there were two experimental evidences [2], possibly caused by the charge transfer effect: 1. the NQR lines ν_{1Q} and ν_{2Q} showed ten times larger width than those usually observed in the single valence Au(III) complexes [6]. 2. ESR spectra confirmed the presence of paramagnetic Au(II) sites in the crystal with an abundance of ca. 5×10^{20} /mol.

Preliminary results of ³⁵Cl quadrupole relaxation time T_{1Q} measurements indicated that the T_{1Q} of both ν_{Q1} and ν_{Q2} were governed by the lattice vibration at low temperatures. However, the T_{1Q} behavior at high temperatures remained uncertain.

The concentration of paramagnetic sites can considerably affect the NQR line width $\Delta\nu$ and T_{1Q} behavior. Therefore we have undertaken further $\Delta\nu$ and T_{1Q} measurements on the same compound, but prepared in a different manner [2], because the Au(II) concentration is expected to depend on the method of preparation. Cs₂[Ag(I)Cl₂][Au(III)Cl₄] has been also prepared for NQR and ESR measurements, because the Ag(I) complex is isostructural with Cs₂-[Au(I)Cl₂][Au(III)Cl₄] and is expected to have more clearly a different Au(II) site concentration.

Experimental

The NQR, ESR, and X-ray diffraction studies were performed on polycrystalline Cs₂[M(I)Cl₂]-[Au(III)Cl₄] (M = Ag, Au). A home made pulsed

Table 1. Lattice constants and interatomic distances of $\text{Cs}_2\text{-(M(I)Cl}_2\text{)[Au(III)Cl}_4\text{]}$ (M = Au and Ag).

Compound	<i>a</i> /pm	<i>c</i> /pm	Cl-Au(III)M(I)··· L/pm	ClAu(III) L/pm	Ref.
Sample I	748(4)	1084(8)	229.5(5)*	299(3)	
Sample II	748(5)	1084(15)	229.5(5)*	300(4)	
Sample III	737(5)	1086(10)	228.5(5)*	293(4)	
$\text{Cs}_2[\text{AuCl}_2][\text{AuCl}_4]$	749(2)	1087(2)	242	298	[3]
$\text{Cs}_2[\text{AuCl}_2][\text{AuCl}_4]$	749.5(1)	1088.0(2)	229.5	300.5	[4, 5]
$\text{Cs}_2[\text{AgCl}_2][\text{AuCl}_4]$	738(2)	1101(2)	230	292	[3]

* The value is estimated from ^{35}Cl NQR frequency vs. bond length plot [2].

spectrometer [7] was used for the observation of ^{35}Cl NQR. The line shape of the resonances was determined by monitoring the spin echo amplitude dependence on the rf frequencies. The pulse sequence $\pi/2-\tau-\pi/2-\tau_e-\pi$ was employed for the measurements of the spin-lattice relaxation time T_{1Q} , in which τ_e was set to ca. 400 μs throughout the experiments. The ESR spectra were recorded on a JEOL JES-FE1XP X-band spectrometer. The X-ray powder patterns were recorded on a model 2012 diffractometer from Rigaku Denki Co., equipped with a copper anticathode.

Two kinds of samples of $\text{Cs}_2[\text{Au(I)Cl}_2][\text{Au(III)Cl}_4]$ [2] were employed for the measurements. One (**I**) was prepared by the Bridgman method [8] and recrystallized by the thermal diffusion method. The other (**II**) was prepared in a similar way as described in [9] and purified by sublimation. $\text{Cs}_2[\text{Ag(I)Cl}_2][\text{Au(III)Cl}_4]$ (**III**) was also prepared as in [9] and used without further purification.

Results and Discussion

X-ray Diffraction and ESR

The diffraction patterns, strongly resembling each other, were observed for the samples **I**, **II**, and **III**. No impurity peaks were observed.

The one-to-one correspondence of the diffraction lines indicated that the crystals of the three samples were isostructural with the space group $I4/mmm$.

The determined tetragonal lattice constants *a* and *c* are given in Table 1. These values are in good agreement with those already reported [3 - 5], except the *c*-axis length of $\text{Cs}_2[\text{Ag(I)Cl}_2][\text{Au(III)Cl}_4]$.

All the samples showed ESR. The appearance of the ESR signals evidences the presence of a

small amount of d^9 paramagnetic sites in the sample crystals. Sample **I** showed a single resonance line arising from Au(II) sites with abundance of ca. $5 \times 10^{20} \text{ mol}^{-1}$ [2]. A similar but much weaker resonance line was observed for **II**, showing a one order of magnitude lower Au(II) concentration. The sample **III** exhibited two peaks with nearly the same intensity on the ESR spectrum. That the spectrum consists of a doublet is attributable to the existence of Ag(II) and Au(II) sites in the crystal. The paramagnetic concentration was nearly the same in **II**.

NQR Frequency and Line Width

The sample **I** showed the ^{35}Cl resonance $\nu_{Q1} = 17.28 \text{ MHz}$ for Au(I)-Cl and $\nu_{Q2} = 27.10 \text{ MHz}$ for Au(III)-Cl at 77 K [2]. The sample **II** yielded the same resonance frequencies as **I**, whereas **III** showed a singlet frequency $\nu_{Q2} = 27.96 \text{ MHz}$ at 77 K attributable to Au(III)-Cl. Experiments to detect the ^{35}Cl NQR of Cl-Ag(I) for **III** have been unsuccessful.

Comprehensive studies have revealed the existence of strong correlations between the ^{35}Cl NQR frequency and the bond lengths C-Cl and Sn-Cl [10]. The NQR frequency vs. bond length plot in various $[\text{Au(III)Cl}_4]^-$ [2] reasonably suggests that the Au(III)-Cl bond length in **III** is 228.5 pm, which is shorter by ca. 1 pm than that in $\text{Cs}_2[\text{Au(I)Cl}_2][\text{Au(III)Cl}_4]$ (Table 1). A reduction on the *a*-axis occurs when Au(I) is substituted by Ag(I). This is likely caused by the smaller ionic radius of Ag(I) resulting in a shorter inter-atomic distance Ag(I)···Cl-Au(III).

The resonance line shapes determined from ^{35}Cl spin echo intensity measurements were Lorentzian [11]. Gaussian fits to the experimental data showed clear deviations. The normalized lines are shown in Figure 1. The lines were temperature independent and much broader than $\Delta\nu_Q \sim 10 \text{ kHz}$ observed for the single valence compound $\text{Cs}[\text{AuCl}_4]$ [6]. The sample **I**, **II** and **III** showed full line widths of 60, 155 and 60 kHz, respectively, at half height. The line width of the sample **I** annealed at 673 K, just below the melting point, was unchanged. The thermal treatment removes adsorbed solvent molecules such as H_2O and HCl from the crystal and releases the crystal from strain. An effect of crystal imperfection, unconnected with the presence of Au(II), was not discernible in the line width of **I**. The presence of Au(II) should be an essential factor for the line broadening because such a broad

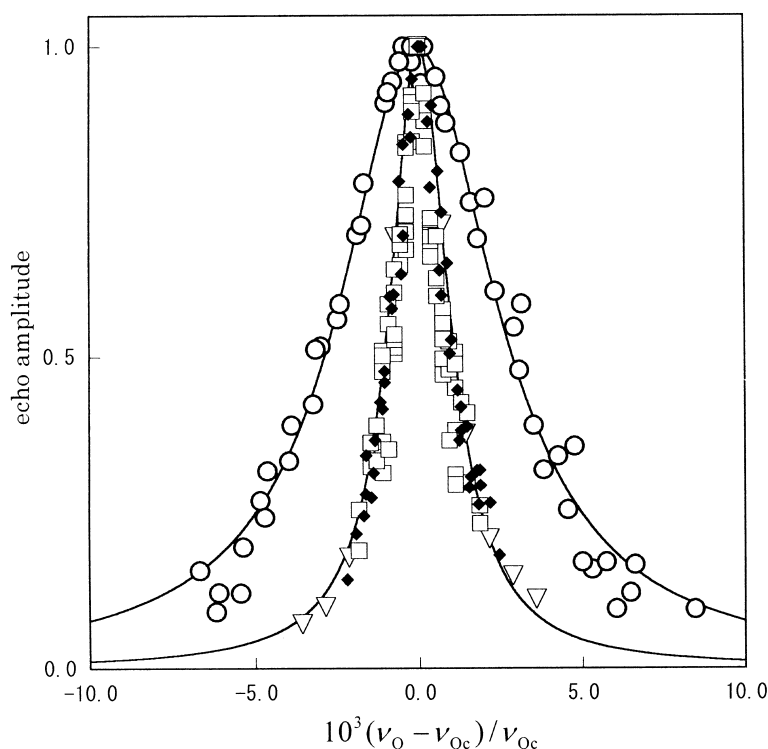


Fig. 1. Echo spectra of ^{35}Cl NQR in $\text{Cs}_2[\text{Au}(\text{I})\text{Cl}_2][\text{Au}(\text{III})\text{Cl}_4]$ and $\text{Cs}_2[\text{Ag}(\text{I})\text{Cl}_2][\text{Au}(\text{III})\text{Cl}_4]$. Solid lines represent the best fitted Lorentzian curves. ν_{Qc} is the center frequency of each resonance. \blacklozenge : ν_{Q1} for sample **I**; \square : ν_{Q2} for sample **I**; \circ : ν_{Q2} for sample **II**; ∇ : ν_{Q2} for sample **III**.

width has not been observed in single valence Au(III) complexes. The sample **II** yielded the widest line in spite of its lowest Au(II) site concentration of the three samples. The problem about the origin of the line broadening has not been yet settled. At least the experimental results suggest that even a small amount of paramagnetic sites, such as ca. $5 \times 10^{19} \text{ mol}^{-1}$, can contribute to the broadening effect, and the excess contents of the sites is irrelevant for this effect.

Librational Motion

The temperature dependence of the ^{35}Cl resonance frequencies is shown in Figure 2. The frequency decrease is attributable to the EFG averaging at Cl due to the librational motion of the complex anions. Since the temperature dependence of ν_Q is almost linear, we can apply the Bayer-Kushida equation in the high temperature limit [12]:

$$[\nu_Q(T) - \nu_{Q0}]/\nu_{Q0} = -\frac{3k}{2I_{\text{eff}}\omega_{\text{eff}}^2}T = -AT, \quad (1)$$

where ν_{Q0} denotes the NQR frequency at a fictitious vibrationless state. The temperature coefficient A is a librational amplitude factor which consists of the

Table 2. ^{35}Cl NQR frequency and librational amplitude factor A in $\text{Cs}_2[\text{M}(\text{I})\text{Cl}_2][\text{Au}(\text{III})\text{Cl}_4]$ ($\text{M} = \text{Au}$ and Ag) at a fictitious vibrationless state ν_{Q0} which fit best with the Bayer-Kushida equation (1).

Sample		ν_{Q0} / MHz	$10^3 A / \text{K}^{-1}$
I	ν_{Q1}	17.45	11.7
	ν_{Q2}	27.16	2.82
II	ν_{Q2}	27.16	2.74
III	ν_{Q2}	28.07	5.23

Boltzmann constant k , an effective moment of inertia I_{eff} and an effective librational frequency ω_{eff} . The values of A and ν_{Q0} which fit (1) best are summarized in Table 2. The small difference of A between **I** and **II** for ν_{Q2} falls within the experimental errors due to the broadness of the resonance lines. The large A for ν_{Q1} results from the large librational amplitude of $[\text{Au}(\text{I})\text{Cl}_2]^-$, which has a smaller I_{eff} than $[\text{Au}(\text{III})\text{Cl}_4]^-$. It is worth to note that ν_{Q1} showed an about four times larger A than ν_{Q2} despite the maximum moment of inertia of $[\text{Au}(\text{III})\text{Cl}_4]^-$ is roughly two times larger than that of $[\text{Au}(\text{I})\text{Cl}_2]^-$, when we consider the motion of the isolated complex anions. Possibly the repulsive force between the Au(I)-Cl chlorine and d_{z^2} electrons on Au(III) contributes to

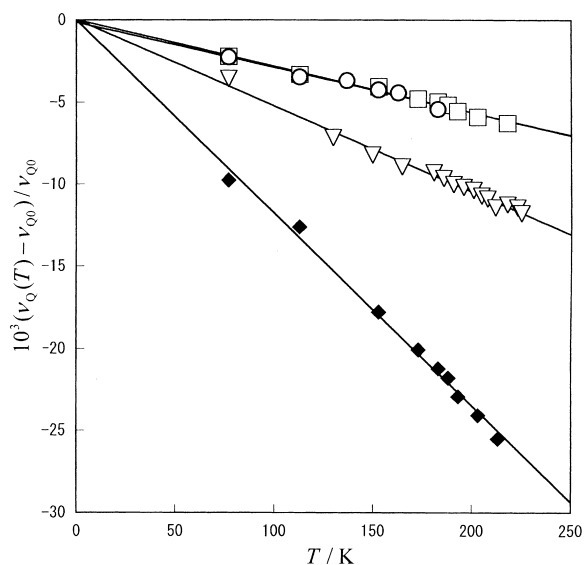


Fig. 2. Temperature dependence of ^{35}Cl NQR frequencies of $\text{Cs}_2[\text{Au}(\text{I})\text{Cl}_2][\text{Au}(\text{III})\text{Cl}_4]$ and $\text{Cs}_2[\text{Ag}(\text{I})\text{Cl}_2][\text{Au}(\text{III})\text{Cl}_4]$. The solid lines are least-squares fits of the data with the Bayer-Kushida equation (1). The resonance frequencies are normalized by the frequency ν_{Q0} at a fictitious rigid state of the lattice vibration. \blacklozenge : ν_{Q1} for sample **I**; \square : ν_{Q2} for sample **I**, \circ : ν_{Q2} for sample **II**, ∇ : ν_{Q2} for sample **III**.

this effect through ω_{eff} . Sample **III** yielded larger A of ν_{Q2} than **I** and **II**. The $d_{x^2-y^2}$ electrons on $\text{Ag}(\text{I})$ will repel more strongly the Cl in $[\text{Au}(\text{III})\text{Cl}_4]^-$ than the electrons on $\text{Au}(\text{I})$.

Spin-lattice Relaxation

The temperature dependence of the ^{35}Cl NQR spin-lattice relaxation times T_{1Q} is displayed in Figure 3. The T_{1Q} of ν_{Q2} for the three samples behaved similarly against temperature variation. At 77 - 180 K the T_{1Q} values were nearly proportional to T^{-2} . At 180 - 220 K, the $\log T_{1Q}$ values were proportional to $1/T$. The temperature dependence of T_{1Q} is expressed [13 - 15] by

$$T_{1Q}^{-1} = aT^n + b \exp(-E_a/RT), \quad (2)$$

where a , n , and b are the parameters relating to the molecular motions including Cl . The first term concerns the lattice vibration and the second term the molecular reorientation over the potential barrier E_a . The motional parameters and E_a which fit best with the experimental data are listed in Table 3. The temperature dependence of T_{1Q} for ν_{Q1} also showed the

Table 3. Motional parameters a , n , b , and E_a for $\text{Cs}_2-[\text{M}(\text{I})\text{Cl}_2][\text{Au}(\text{III})\text{Cl}_4]$ ($\text{M} = \text{Au}$ and Ag).

Sample		$10^4 a / (\text{s}^{-1} \text{K}^{-n})$	n	$10^{-11} b / \text{s}^{-1}$	$E_a / (\text{kJ mol}^{-1})$
I	ν_{Q1}	1.2	2.1		
I	ν_{Q2}	1.3	2.2	1.4	34
II	ν_{Q2}	1.8	2.7	1.6	34
III	ν_{Q2}	4.0	2.1	2.4	37

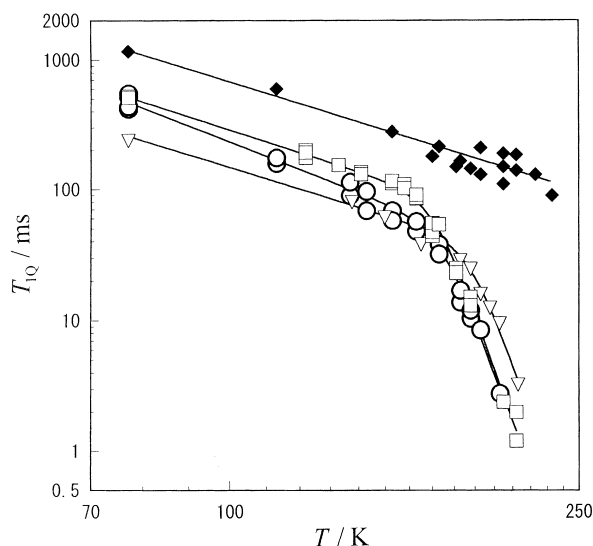


Fig. 3. Temperature dependence of the ^{35}Cl NQR spin-lattice relaxation times T_{1Q} of $\text{Cs}_2[\text{Au}(\text{I})\text{Cl}_2][\text{Au}(\text{III})\text{Cl}_4]$ and $\text{Cs}_2[\text{Ag}(\text{I})\text{Cl}_2][\text{Au}(\text{III})\text{Cl}_4]$. The solid lines represent the best fitted theoretical curve (2). \blacklozenge : ν_{Q1} for sample **I**; \square : ν_{Q2} for sample **I**, \circ : ν_{Q2} for sample **II**, ∇ : ν_{Q2} for sample **III**.

T^{-2} behavior at lower temperatures. However, no further activation process was observed even at higher temperatures.

Relaxation Mechanism and Conservation of Gold Valence

The concentration of $\text{Au}(\text{II})$ for **I** was ten times larger than that for **II**. However, a similar temperature dependence of T_{1Q} was observed on both samples for ν_{Q2} . The small T_{1Q} difference arises mainly from the different values of the parameters a and n , both of which depend directly on the lattice vibration. The presence of the $\text{Au}(\text{II})$ site in the crystal may affect the lattice vibration, but the magnitude of the effect is unknown. In the high temperature region 180 - 220 K, the T_{1Q} values of ν_{Q1} and ν_{Q2} were fairly different. This indicates that the ^{35}Cl NQR spin-lattice relax-

ation takes place respectively within a single anion $[\text{Au(I)Cl}_2]^-$ or $[\text{Au(III)Cl}_4]^-$. The Au(II) diffusion process is not observable in the T_{1Q} behavior. The diffusion causes the jumping of electrons between $[\text{Au(I)Cl}_2]^-$ and $[\text{Au(III)Cl}_4]^-$, which will equalize the T_{1Q} of both ν_{Q1} and ν_{Q2} . As an independent relaxation mechanism, reorientation of $[\text{Au(III)Cl}_4]^-$ around the C_4 axis is responsible for the T_{1Q} of ν_{Q2} in the high temperature range. The samples **I** and **II** yielded the same E_a for the reorientation. The sample **III** showed a close value to those of **I** and **II**. For ν_{Q1} the lattice vibrations govern the relaxation in the whole temperature range. The temperature dependence of T_{1Q} for the three samples is well described by (2), in which only the effects of the lattice vibration

and reorientational motion of the complex anions are taken into account. Furthermore, samples having different paramagnetic concentrations yielded the similar motional parameters for ν_{Q2} . Therefore it is concluded that the charge transfer interaction between the anions is unchanged and no additional formation of paramagnetic sites is allowed for these mixed-valence complexes in the temperature range studied. This conclusion is also supported by the fact that the temperature dependence of the signal intensity of the ESR signals obeyed Curie's law for **I** [2].

Acknowledgement

We appreciate the experimental assistance of Mr. M. Kano in recording the ESR spectra.

- [1] N. Kojima, Bull. Chem. Soc. Japan **73**, 1445 (2000).
- [2] A. Ishikawa, M. Kurasawa, S. Kitahara, A. Sasane, N. Kojima, and R. Ikeda, Z. Naturforsch. **53a**, 590 (1998).
- [3] N. Elliot and L. Pauling, J. Amer. Chem. Soc. **60**, 1846 (1938).
- [4] J. C. M. Tindemans-v. Eindhoven and G. C. Verschoor, Mater. Res. Bull. **9**, 1667 (1974).
- [5] D. Denner, H. Schulz, and H. d'Amour, Acta Cryst. **35A**, 360 (1979).
- [6] A. Ishikawa, T. Asaji, D. Nakamura, and R. Ikeda, Z. Naturforsch. **44a**, 125 (1989).
- [7] A. Sasane, M. Shinha, Y. Hirakawa, and A. Ishikawa, J. Mol. Struct. **345**, 205 (1995).
- [8] H. Kitagawa, N. Kojima, N. Matsushita, T. Ban, and I. Tsujikawa, J. Chem. Soc. Dalton Trans. **1991**, 3115.
- [9] H. L. Wells, Amer. J. Sci. **3**, 315 (1922).
- [10] Al. Weiss and S. Wigand, Z. Naturforsch. **45a**, 195 (1990).
- [11] K. Horiuchi, R. Ikeda, and D. Nakamura, Ber. Bunsenges. Phys. Chem. **91**, 1351 (1987).
- [12] T. Kushida, G. B. Benedek, and N. Bloembergen, Phys. Rev. **104**, 1364 (1956).
- [13] S. Alexander and A. Tzalmona, Phys. Rev. **A138**, 845 (1965).
- [14] K. R. Jeffrey and R. L. Armstrong, Phys. Rev. **174**, 359 (1968).
- [15] H. Chihara and N. Nakamura, Adv. Nucl. Quadrupole Reson. **4**, 1 (1980).